THE JOURNAL OF BIOLOGICAL CHEMISTRY VOL. 290, NO. 4, pp. 2150–2165, January 23, 2015

Molecular Basis of the Dominant Negative Effect of a Glycine Transporter 2 Mutation Associated with Hyperekplexia*

Received for publication, June 6, 2014, and in revised form, December 4, 2014 Published, JBC Papers in Press, December 5, 2014, DOI 10.1074/jbc.M114.587055

Esther Arribas-González[‡§], Jaime de Juan-Sanz[‡§¶1], Carmen Aragón[‡§¶], and Beatriz López-Corcuera[‡§¶2]

From the [‡]Departamento de Biología Molecular and Centro de Biología Molecular "Severo Ochoa," Consejo Superior de Investigaciones Científicas-Universidad Autónoma de Madrid, Madrid 28049, Spain, the [¶]Centro de Investigación Biomédica en Red de Enfermedades Raras, Instituto de Salud Carlos III, Madrid 28029, Spain, and the [§]IdiPAZ-Hospital Universitario La Paz, Universidad Autónoma de Madrid, Madrid 28046, Spain

Background: Hyperekplexia is caused by defective glycinergic neurotransmission.
Results: A dominant negative glycine transporter-2 mutant is trapped in a calnexin-bound state and retains wild type GlyT2 in the endoplasmic reticulum.
Conclusion: Chemical chaperones rescue the folding defect of the mutant and overcome its dominant negative effect.
Significance: This opens the way to revert the dominant negative effect exerted by the mutant associated with hyperekplexia in neurons.

Hyperekplexia or startle disease is a rare clinical syndrome characterized by an exaggerated startle in response to trivial tactile or acoustic stimuli. This neurological disorder can have serious consequences in neonates, provoking brain damage and/or sudden death due to apnea episodes and cardiorespiratory failure. Hyperekplexia is caused by defective inhibitory glycinergic neurotransmission. Mutations in the human *SLC6A5* gene encoding the neuronal GlyT2 glycine transporter are responsible for the presynaptic form of the disease. GlyT2 mediates synaptic glycine recycling, which constitutes the main source of releasable transmitter at glycinergic synapses. Although the majority of GlyT2 mutations detected so far are recessive, a dominant negative mutant that affects GlyT2 trafficking does exist. In this study, we explore the properties and structural alterations of the S512R mutation in GlyT2. We analyze its dominant negative effect that retains wild-type GlyT2 in the endoplasmic reticulum (ER), preventing surface expression. We show that the presence of an arginine rather than serine 512 provoked transporter misfolding, enhanced association to the ER-chaperone calnexin, altered association with the coat-protein complex II component Sec24D, and thereby impeded ER exit. The S512R mutant formed oligomers with wild-type GlyT2 causing its retention in the ER. Overexpression of calnexin rescued wild-type GlyT2 from the dominant negative effect of the mutant, increasing the amount of transporter that reached the plasma membrane and dampening the interaction between the wild-type and mutant GlyT2. The ability of chemical chaperones to overcome the dominant negative effect of the disease mutation on the wild-type transporter was demonstrated in heterologous cells and primary neurons.

The extracellular concentration of synaptic glycine is regulated by Na^+-and Cl^--dependent glycine reuptake (1). The neuronal GlyT2 transporter is involved in the removal and recycling of glycine from inhibitory synapses, generating a flux from the synaptic cleft to the presynaptic terminal and supplying substrate to the low affinity vesicular inhibitory amino acid transporter (2, 3). Therefore, the synaptic glycine taken up by GlyT2 is the main source of the releasable transmitter at glycinergic synapses (4, 5). Accordingly, inactivation of the mouse GlyT2 gene generates a complex postnatal neuromotor phenotype that mimics clinical signs of human hyperekplexia (2).

Hyperekplexia or startle disease (OMIM 149400) is a rare neurological disorder characterized by neonatal hypertonia and exaggerated startle responses to trivial but unexpected tactile or acoustic stimuli (6). The most severe consequences of the disease include brain damage and even sudden death from lapses in cardiorespiratory function. Although the majority of patients survive, they may suffer unprotected falls throughout their entire life that could result in injury (7). Startle disease is a glycinergic synaptopathy that disrupts postsynaptic or presynaptic inhibitory glycinergic neurotransmission. The main genes implicated in startle disease are those corresponding to the glycine receptor and related postsynaptic proteins (8, 9), with genetic analyses revealing mutations in the human GlyT2 gene (*SLC6A5*; solute carrier 6A5) to be the most common cause of presynaptic hyperekplexia (10–12) and a very common cause of the disease. The majority of GlyT2 mutations found in hyperekplexia patients are recessive and cause biallelic loss of function due to the absence of the protein from the plasma membrane or to the generation of inactive transporters. Recently, a dominantly inherited mutation affecting the function that also reduces the expression of the transporter at the cell membrane was identified and characterized (13). In addition, one interesting mutation is S512R, the sole dominant negative disease-as-

* This work was supported by Spanish "Ministerio de Economia y Competitividad" Grant SAF2011-28674, by the Centro de Investigación Biomédica en Red de Enfermedades Raras (CIBERER), and by an institutional grant from the "Fundación Ramón Areces."
[1] Present address: Dept. of Biochemistry, Weill Cornell Medical College, New York, NY 10065.
[2] To whom correspondence should be addressed: Dept. de Biología Molecular, Centro de Biología Molecular "Severo Ochoa", Universidad Autónoma de Madrid, 28049 Madrid, Spain. Tel.: 34-91-1964631; Fax: 34-91-1964420; E-mail: blopez@cbm.csic.es.

sociated mutation affecting transporter trafficking. This mutant transporter prevents the wild-type protein from reaching the plasma membrane, although its exact mechanism of action has yet to be fully defined (10).

GlyT2 belongs to the SLC6 solute carrier family of neurotransmitter sodium symporters. This family groups together 12-transmembrane domain transport proteins including the GABA (γ-aminobutyric acid) and monoamine transporters (14, 15). A model of the three-dimensional structure of GlyT2 was recently generated (16) based on the leucine transporter from *Aquifex aeolicus* ($LeuT_{Aa}$), a prokaryotic SLC6 homologue (18). This model provided important clues to explain the effects of selected missense mutations on critical residues involved in Na^+ and glycine binding (8, 10–13). More recently, the crystal structure of a eukaryotic SLC6, the dopamine transporter (DAT)[3] from *Drosophila*, was resolved (19). Among the differences from the prokaryotic model, the presence of a cholesterol binding site is particularly relevant in the context of DAT and GlyT2, which are lipid-raft-associated transporters (20).

During GlyT2 synthesis, the nascent polypeptide is co-translationally translocated to the membrane of the endoplasmic reticulum (ER) (21). Correct folding of the transporter is stabilized by its four *N*-glycan chains, but it also requires an interaction with several ER chaperones (22). For example, calnexin (CNX) transiently binds to an intermediate hypoglycosylated transporter precursor, and it facilitates GlyT2 processing. The binding of GlyT2 to CNX is mediated by glycan- and polypeptide-based interactions, allowing CNX to discriminate between different GlyT2 conformational states through a lectin-independent chaperone activity (23, 24). In addition, oligomer assembly is a prerequisite to export the SLC6 transporters from the ER and for their subsequent delivery to the plasma membrane (25). Accordingly, a model has been proposed in which transporter intermediates are engaged by ER chaperones, and they are delivered to the coatomer protein II (COPII) prior to forming oligomers that can subsequently be exported out of the ER (25, 26). In the present study, we characterize the features and behavior of the dominant negative hyperekplexia mutant in the early secretory pathway. We confirmed its dominant negative effect on the trafficking of wild-type GlyT2 by means of an interaction in common oligomers. We found that this mutant transporter provoked the retention of the wild-type GlyT2 in the ER, an effect that could be reverted by the overexpression of CNX. An excess of this chaperone increased the amount of wild-type transporter that reaches the plasma membrane by preventing the interaction between wild-type and mutant GlyT2. The effect of pharmacological chaperones in the rescue of GlyT2 was analyzed in heterologous cells and transfected cortical neurons.

EXPERIMENTAL PROCEDURES

Cell Growth and Protein Expression—COS7 cells (American Type Culture Collection) were grown at 37 °C and 5% CO_2 in Dulbecco's modified Eagle's medium (DMEM) supplemented with 10% fetal bovine serum. Transient expression was achieved using Neofectin™ (MidAtlantic Biolabs), according to the manufacturer's protocol (24), and the cells were then incubated for 48 h at 37 °C. Reproducible results were obtained with 50–60% confluent cells on 60-mm or 6-well plates, using 5 and 2 μg of total DNA, respectively. In co-transfection experiments, 25% of the total DNA was wild-type DNA. The transfection efficiency was determined by co-transfecting the cDNAs with the pSV-β-galactosidase plasmid (Promega) and measuring β-galactosidase activity 24 h later, as described elsewhere (24).

Plasmid Constructs—The pRFP vector (27) was a generous gift of José Antonio Esteban (Centro de Biología Molecular Severo Ochoa, Madrid, Spain). The Myc-Sec24D and HA-GlyT2 constructs in the pcDNA3 plasmid (Invitrogen) were generously provided by Francisco Zafra (Centro de Biología Molecular Severo Ochoa). GlyT2 (28) was subcloned into pcDNA3 or pRFP (BglII-SalI sites), and the GlyT2 mutants were constructed by site-directed mutagenesis using the QuikChange kit (Stratagene) (29). S512R was subcloned in the unique EcoRI and XbaI sites flanking HA-GlyT2. The complete coding region of all of the constructs was sequenced to verify that only the desired mutation had been introduced. Plasmids from two independent *Escherichia coli* colonies were transfected into eukaryotic cells, and [^{3}H]glycine transport was measured in the cells for verification. The GFP-GlyT2 plasmid was constructed and characterized as described previously (30, 31). The RFP and HA tags were fused in frame with GlyT2 at the N terminus, and they did not interfere either with the uptake capacity in [^{3}H]glycine uptake assays or its expression at the plasma membrane as assessed by biotinylation (see Fig. 5*A*). C-terminal tagging was avoided because previous reports indicated that this region of the transporter might be involved in specific interactions and intracellular trafficking (32). The CNX cDNA clone (IMAGE number 2582119) in pCMV.SPORT6 was purchased from Source Bioscience Lifesciences (24).

Transport Assays—Glycine transport assays on COS7 cells were performed at 37 °C in phosphate-buffered saline (PBS) containing 10 mM glucose and 2 μCi/ml 2-^{3}H-labeled glycine (1.6 TBq/mmol; PerkinElmer Life Sciences), diluted to a final concentration of 10 μM, as described previously (24). For glutamate transport assays, the radiolabeled glycine was substituted with the same amount of ^{3}H-labeled glutamate. These reactions were run for 10 min and then terminated by aspiration. The protein concentration was determined in aliquots taken from each well (Bradford), and the uptake of [2-^{3}H]glycine was measured by liquid scintillation (LKB 1219 Rackbeta). Transport was quantified by subtracting the glycine accumulated in mock-transfected COS7 cells (or in the presence of the specific GlyT2 inhibitor, ALX1393) from that of the transporter-transfected cells and normalized to the protein concentration. Assays were performed in triplicate or quadruplicate.

Surface Biotinylation—COS7 cells expressing wild type or mutant GlyT2 were grown in 6-well plates (Nunc), washed, and labeled with Sulfo-NHS-Biotin (1.0 mg/ml in PBS; Pierce) at 4 °C, a temperature that blocks membrane trafficking of proteins. After quenching with 100 mM L-lysine to inactivate the

[3] The abbreviations used are: DAT, dopamine transporter; CNX, calnexin; COPII, coatomer protein II; ER, endoplasmic reticulum; ERAD, ER-associated degradation; MDCK, Madin-Darby canine kidney; PBA, sodium 4-phenylbutyrate; TM, transmembrane domain; ANOVA, analysis of variance.

free biotin, the cells were lysed with 1× lysis buffer as described elsewhere (24). A portion of the lysate was saved to determine the total protein content, and the remainder was incubated with streptavidin-agarose beads for 2 h at room temperature with rotary shaking. After centrifugation, the supernatant was removed, and an aliquot was used to quantify the non-biotinylated fraction. The agarose beads recovered were washed three times with 1× lysis buffer, and the bound proteins (biotinylated) were eluted with Laemmli buffer (65 mM Tris, 10% glycerol, 2.3% SDS, 100 mM DTT, 0.01% bromphenol blue) for 10 min at 75 °C. The samples were then analyzed in Western blots.

Immunofluorescent Staining of Cultured Cells—Immunocytochemistry was performed as described (31). Briefly, MDCK II cells, COS7 cells, or primary neurons were fixed with 4% paraformaldehyde in PBS, washed three times with 1 ml of PBS, and then blocked for 30 min with 10% serum in TNT (0.1 M Tris/HCl (pH 7.5), 0.3 M NaCl, and 0.2% Triton X-100). The cells were then incubated for 2 h with the desired primary antibodies (E-cadherin (rat, 1:200), CNX (rabbit, 1:500), GFP (mouse, 1:200), or RFP (rabbit, 1:1000)) diluted in TNT containing 1% serum (TNT-S), after which they were washed three times with TNT buffer and incubated for 2 h with the appropriate secondary antibody diluted in TNT-S (anti-mouse Alexa Fluor 488 (1:200), anti-rabbit Alexa Fluor 555 (1:200), or anti-rat or anti-rabbit Alexa Fluor 647 (1:200)). After three washes with TNT, the coverslips were mounted on microscope slides with Vectashield (Vector Laboratories, Burlingame, CA), and the cells were visualized by confocal microscopy on an inverted microscope AXIOVERT200 (Zeiss). At least 30 images for each condition were quantified using ImageJ software (National Institutes of Health) (as in Ref. 33). The images were processed with a 2.0-pixel median filter, and the threshold applied was automatically determined by the JACoP plugin (34). Pearson's value of correlation was obtained with JACoP by comparing the two thresholded channels and measuring the correlation between them. The value can range from −1 to 1, the latter representing maximal co-localization (two identical images).

Electrophoresis and Western Blotting—Protein samples were separated by SDS-PAGE using a 4% stacking gel and 6 or 7.5% resolving gels. The samples were transferred to nitrocellulose (Invitrogen) (1.2 mA/cm^2 for 2 h), and the membranes were then blocked for 4 h with 5% milk in PBS at 25 °C. The membranes were probed overnight at 4 °C with the desired primary antibody: anti-GlyT2 (rabbit, 1:1,000) (35); anti-GlyT2 (rat, 1:500) (36); anti-CNX (1:1,000; Stressgen Biotechnologies Corp.); anti-ubiquitin (P4D1, 1:200; Santa Cruz Biotechnology, Inc.); anti-HA (monoclonal antiserum 12CA5, 1:500; Sigma); anti-GFP (green fluorescent protein, 1:1,000; Invitrogen); or anti-RFP (red fluorescent protein, 1:2,000; a generous gift of José María Requena, Centro de Biología Molecular Severo Ochoa). After several washes, the antibodies bound were detected with peroxidase-coupled anti-rat (1:8,000; Sigma) or anti-rabbit IgG (1:10,000; Bethyl), which were visualized by enhanced chemiluminescence (ECL; Amersham Biosciences). Subsequently, the antibodies were stripped from the membrane (Thermo Scientific), which was reprobed with anti-tubulin (1:3,000; Sigma), and antibody binding was detected with a peroxidase-coupled anti-mouse IgG. The protein bands were quantified by densitometry.

Carbohydrate Modification—COS7 cells expressing GlyT2 or the desired mutants were lysed in 1× lysis buffer (150 mM NaCl, 50 mM Tris-HCl (pH 7.4), 5 mM EDTA, 1% Triton X-100, 0.1% SDS, 0.25% deoxycholate sodium, 0.4 mM PMSF, and 4 μM pepstatin) and digested with the chosen endoglycosidase (peptide:*N*-glycosidase F (New England Biolabs) or endoglycosidase H or D (Roche Applied Science)) in a small volume of the appropriate buffer, according to the manufacturer's instructions. These cell extracts were then resolved by SDS-PAGE and analyzed in Western blots.

Immunoprecipitation Assays—Transfected COS7 cells were washed twice with PBS and scraped off of the plates in 150 mM NaCl, 50 mM Tris-HCl (pH 7.4), 0.4 mM PMSF, and 4 μM pepstatin, and the desired amount of protein (Bradford method, Bio-Rad) was solubilized for 30 min at 22 °C in lysis buffer with 0.2% Nonidet P-40. After a 15-min centrifugation at 10,000 × *g*, an aliquot of the lysate was retained to measure the total protein content, and the remainder was precleared by adding 20 μl of 50% protein A or G Sepharose (Sigma) in lysis buffer for 30 min at 4 °C with rotation. After centrifugation, the supernatants were incubated overnight at 4 °C with 2 μg of the desired primary antibody, whereas controls with no antibody were also included. Subsequently, 20 μl of protein A or G-Sepharose beads were added to the samples, and after incubating for 1 h at 4 °C, the beads were washed twice for 5 min with 500 μl of 1× lysis buffer. The bound proteins were then dissociated from the beads by heating at 75 °C for 15 min, resolved by SDS-PAGE, and analyzed in Western blots. Sequential immunoprecipitations were performed as described elsewhere (24). Beads containing anti-CNX immunoprecipitated proteins were incubated with 150 μl of 1% SDS in HEPES-buffered saline at 75 °C for 30 min and centrifuged. The supernatant was then diluted with 1.35 ml of 1% CHAPS in HEPES-buffered saline (final SDS concentration, 0.1%), transferred to a new tube, and incubated with an anti-GlyT2 antibody (1.5 μg) overnight at 4 °C. The immunocomplexes formed were again recovered with fresh beads, eluted, and analyzed as above.

Pulse-Chase Experiments—Cells cultured to 80–90% confluence in p60 or p100 plates were maintained in methionine-free medium for 1 h prior to performing the pulse-chase experiments (24). The cells were then pulse-labeled for 15 min with 0.25 mCi/ml [^{35}S]methionine/cysteine (Redivue Promix, Amersham Biosciences) and chased for varying periods in DMEM + 10% fetal calf serum (FCS) containing 1 mM cycloheximide to quickly stop the elongation of nascent polypeptide chains. Labeling was quenched by the addition of ice-cold PBS containing 20 mM freshly prepared *N*-ethylmaleimide to prevent the oxidation of free sulfhydryl groups. The proteins were immunoprecipitated from the cell lysates with a GlyT2 antibody (35) or sequentially with anti-CNX (Stressgen) and anti-GlyT2 antibodies as described above. The samples were resolved by SDS-PAGE, fixed, and treated with Amplify fluorography reagent (Amersham Biosciences). The gels were dried and exposed for 4–12 days at −70 °C, and the protein bands were quantified by densitometry.

Primary Cultures of Cerebral Cortex—Primary cultures of embryonic cortical neurons were prepared as described previously (37). Briefly, the cortex of Wistar rat fetuses was obtained on the 18th day of gestation, and the tissue was mechanically disaggregated in Hanks' balanced salt solution (Invitrogen) containing 0.25% trypsin (Invitrogen) and 4 mg/ml DNase (Sigma). Cells were plated at a density of 500,000 cells/well in 6-well plates (Falcon), and they were incubated for 4 h in DMEM + 10% FCS, containing glucose (10 mM), sodium pyruvate (10 mM), glutamine (0.5 mM), gentamicin (0.05 mg/ml), streptomycin (0.1 mg/ml), and penicillin G (6×10^{-5} mg/ml). After 4 h, the buffer was replaced with Neurobasal/B27 culture medium containing glutamine (0.5 mM, 50:1 by volume; Invitrogen), and 3 days later, cytosine arabinoside ($2.5–5 \times 10^{-3}$ mM) was added to inhibit further glial growth. For transfection, neurons that had been maintained *in vitro* for 7 days were incubated with 2 μg of total DNA mixed with 4 μl of Lipofectamine 2000 reagent (Invitrogen). GlyT2 glycine transport and membrane expression were measured after 48 h in culture.

Densitometry and Data Analysis—The protein bands visualized by ECL (Amersham Biosciences) or fluorography were quantified in a GS-800 calibrated imaging densitometer using the Bio-Rad Quantity One software, with film exposures in the linear range. Non-linear regression fits of experimental transport data were performed using ORIGIN software (Microcal Software, Northampton, MA). The *error bars* represent the S.E. of at least triplicate samples, and the representative experiments shown were repeated no fewer than three times with comparable results.

RESULTS

S512R Exerts a Dominant Negative Effect on the Wild-type GlyT2—Scanning the 16 coding exons of the human GlyT2 gene (*SLC6A5*) in a cohort of hyperekplexia patients recently revealed a missense mutation in exon 10 associated with dominant autosomic inheritance (10). This mutation yields a protein with a serine to arginine substitution in transmembrane domain 7 (S512R), for which a dominant negative role on GlyT2 trafficking was proposed. To characterize this effect, we expressed the recombinant S512R mutant together with the wild-type GlyT2 in eukaryotic cells, and we measured the mutant's effect on GlyT2 membrane expression and on glycine transport (Fig. 1). We employed an optimized co-transfection protocol that makes use of low amounts of cDNA to avoid saturating the cell's translation machinery (see "Experimental Procedures"). Accordingly, only specific effects were observed that allowed us to characterize the dominant negative behavior of the mutant.

As we reported previously (24), when expressed in heterologous cells, GlyT2 appears as a doublet of two protein bands in Western blots; the mature transport-competent form that is present at the plasma membrane migrated as a 100 kDa band, and the immature hypoglycosylated transporter appeared as a 75-kDa protein band. When the S512R mutant was expressed heterologously, no 100 kDa band was evident in Western blots, and the molecular weight of the sole protein band detected was compatible with that of the 75-kDa immature form (Fig. 1*A*). Thus, it was not surprising that the S512R transporter was inactive. Indeed, when the mutant was co-expressed with the wild-type GlyT2, the amount of the 100 kDa band and glycine transport were both reduced to 42.1 ± 4.5 and 51.0 ± 5.3% (mean ± S.E.) of the original values, respectively. Furthermore, the surface mature wild-type transporter available for biotinylation was reduced in a dose-dependent manner when co-expressed with increasing amounts of S512R mutant. Thus, equal amounts of wild-type and mutant DNA (1:1 condition) caused the wild-type surface expression to decrease to 43.1 ± 2.2% (biotinylated GlyT2) and glycine transport to decrease to 37.1 ± 2.2% of their original values (Fig. 1, *B* and *C*), whereas 2- and 3-fold increases in the concentration of co-expressed mutant (1:2 and 1:3 conditions) produced further reductions in membrane expression (to 24.5 ± 2.3 and 18.6 ± 1.6%, respectively) and in transport activity (to 21.5 ± 1.8 and 14.8 ± 1.7%, respectively). By contrast, when wild-type GlyT2 was expressed together with increasing amounts of another inactive GlyT2 mutant (G485C) that reached the plasma membrane normally, glycine transport was unaltered (Fig. 1, *B* and *D*). Likewise, when increasing concentrations of S512R were co-expressed with the non-related GLT1 (glutamate transporter 1), neither GLT1 plasma membrane expression nor the transport of glutamate was affected (Fig. 1, *B* and *E*). These results confirm a dominant negative role of S512R on wild-type GlyT2 and indicate that the mutant acts specifically on the wild-type GlyT2. Besides, this behavior is not a general feature of GlyT2 mutants but rather a particular property of S512R.

The ability of S512R to reduce the amount of wild-type GlyT2 at the cell surface was also monitored in MDCK cells through its co-localization with the plasma membrane marker E-cadherin (Fig. 1*F*). For this purpose, we used constructs of wild-type and mutant fused to N-terminal tags. The tags did not interfere with either glycine uptake or with the plasma membrane expression of the fusion proteins (see Fig. 5*A*). We co-expressed the wild-type and mutant GlyT2 fused to GFP or RFP, and we analyzed the cells by immunofluorescence to detect E-cadherin. The images show that the RFP-S512R fusion protein was clearly absent from the plasma membrane, and the presence of the mutant strongly diminished the surface expression of the wild-type GFP-GlyT2. Thus, the co-localization of GFP-GlyT2 with E-cadherin was reduced to 50.4 ± 2.5% when it was co-expressed with RFP-S512R rather than with RFP-GlyT2 (*right histogram*). Therefore, the GFP- or RFP-tagged (or HA-tagged) transporter constructs reproduced the dominant negative behavior of the mutant transporter as well as replicating the properties of the wild-type transporter.

S512R Characterization—The failure to detect a mature S512R transporter suggests that the missense mutation prevents the progression along the secretory pathway. To determine whether the removal of the serine or the introduction of the arginine impeded post-translational processing of the transporter, we evaluated multiple amino acid substitutions at position 512 (Fig. 2*A*). Surface biotinylation of the mutants expressed in COS7 cells led us to conclude that the lack of a mature transporter at the cell surface was due to the introduction of the arginine. Indeed, this feature was also observed for a similar substitution at the contiguous position 511, where the presence of an arginine residue also impaired the production of

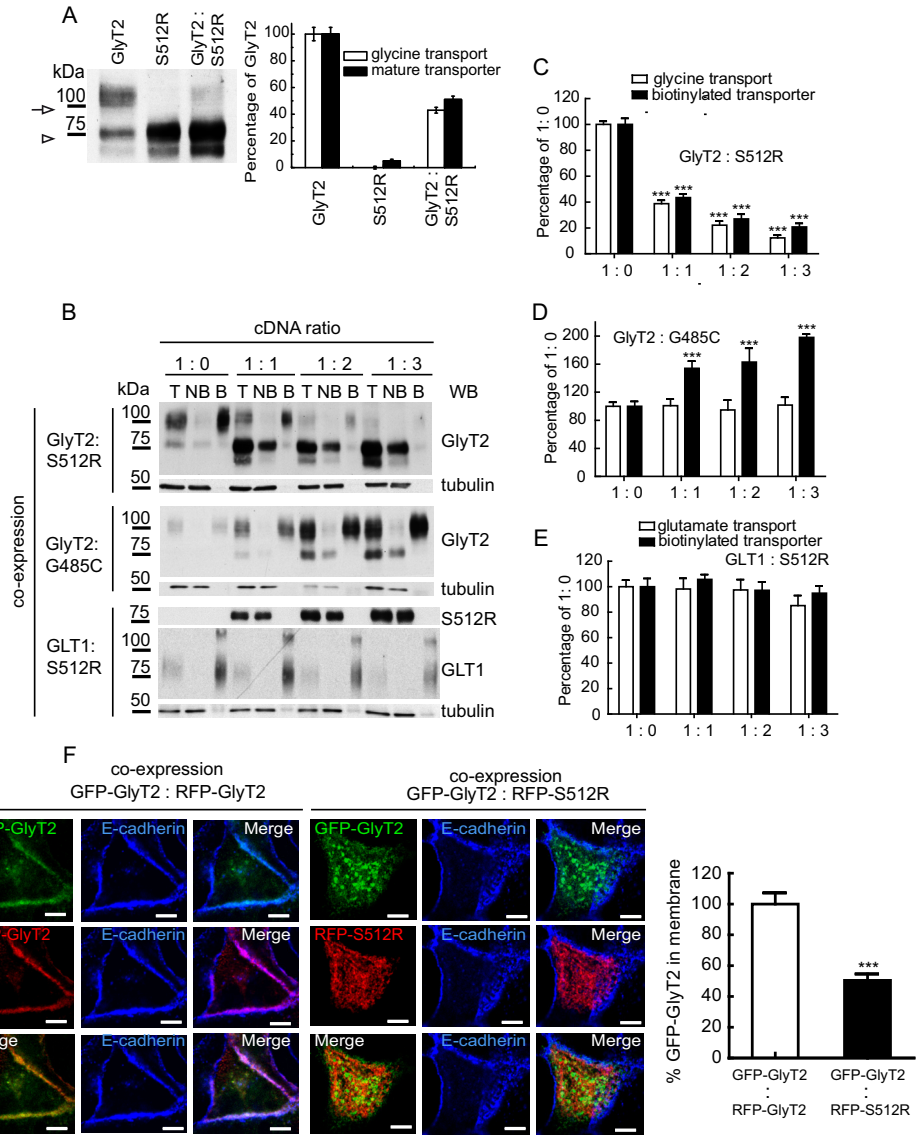

FIGURE 1. **S512R mutant has a dominant negative effect on GLYT2 trafficking.** *A*, COS7 cells expressing GlyT2, S512R, or both (1:1 cDNA ratio, by weight) were assayed in Western blots (*left*) and for glycine transport (*right*). The 100-kDa mature transporter in the Western blot (*arrow*) was densitometered and is represented together with the measured transport activity (*right*). The 75 kDa immature band is labeled with an *arrowhead*. 100% GlyT2 glycine transport was 3.3 ± 0.6 nmol/mg of protein/10 min (mean ± S.E.). *B–E*, COS7 cells were transfected with the wild-type GlyT2 cDNA alone or co-transfected with increasing amounts of S512R cDNA to reach the indicated GlyT2/S512R cDNA ratios (by weight) and then assayed by biotinylation (*B*) and for glycine transport. *T*, total transporter; *B*, biotinylated transporter; *NB*, non-biotinylated transporter. Western blots (*WB*) were reprobed for tubulin as a loading control. *C–E*, 100% glycine and glutamate transport (in nmol/mg of protein/10 min): 3.7 ± 0.5 and 1.2 ± 0.1, respectively (means ± S.E.); ***, $p < 0.001$ with respect to wild-type (ANOVA with Tukey's post hoc test). *F*, MDCK cells expressing the transporters indicated for 48 h were immunolabeled for the plasma membrane marker E-cadherin (*blue*). Three-channel confocal images were obtained (*green* or *red* for transporter and *blue* for E-cadherin), and the regions occupied by E-cadherin were considered as the plasma membrane when using the ImageJ ROI manager, whereas the regions inside the cadherin staining were considered intracellular compartments. After applying an automatic threshold for adjustment, fluorescence intensity was measured separately for membrane and intracellular regions, and the proportion of the transporter at the plasma membrane was calculated (*histogram*). This process was performed in at least 50 cells/condition, representing the means ± S.E. (*error bars*); ***, $p < 0.001$ (Student's *t* test compared with GFP-GlyT2/RFP-GlyT2).

the mature transporter and glycine transport. By contrast, other substitutions were permissive for processing and activity, and although the transport activity of alanine and cysteine mutants was about half that of the wild type, only the serine to threonine mutation restored (and even improved) glycine transport (Fig. 2*A*, *right histogram*). Glycine transport by Ser-512 mutants did not fully correlate with membrane expression, implying that the substitutions affect the activity of surface transporters in addition to their processing. This was predictable because Ser-512 is close to the Na1-coordinating residue, Asn-511. Notably, a serine substitution has been found at this adjacent site associated with hyperekplexia (N511S), yielding a mutant that is almost completely inactive but that reaches the cell surface (10).

We next studied the glycosylation state of the S512R mutant to determine its location in the secretory pathway (Fig. 2*B*). Treating cell lysates expressing wild-type GlyT2 with peptide: *N*-glycosidase F completely removed the *N*-linked glycans from both the 75- and 100-kDa forms, yielding a 60 kDa band. This corresponded to the non-glycosylated protein core because its apparent size coincided with that of the N1234D mutant that lacks the four *N*-glycosylation motifs (24). The mature 100 kDa

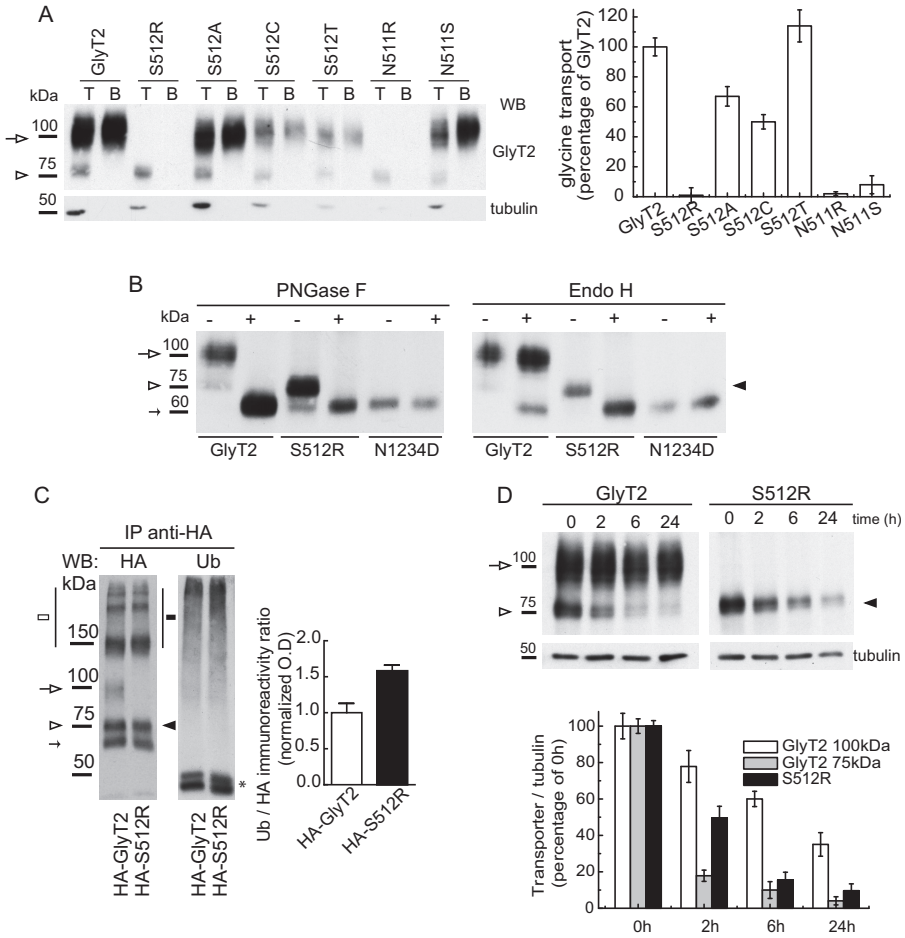

FIGURE 2. **Characterization of the S512R mutant.** *A*, substitution analysis of Ser-512. Shown are biotinylation (*left*) and glycine transport (*right*) of COS7 cells expressing wild-type GlyT2 or mutants with the amino acids indicated at position 512. *T*, total transporter; *B*, biotinylated transporter. Wild-type 100% glycine transport was 3.0 ± 0.6 nmol/mg of protein/10 min (mean ± S.E. (*error bars*)). *B*, carbohydrate modification of S512R. Lysates of COS7 cells expressing the indicated transporters were treated overnight with the vehicle alone (endoglycosidase buffer, −) or with the indicated endoglycosidase (+) in denaturing conditions and then resolved by SDS-PAGE as described under "Experimental Procedures." *C*, the S512R mutant is ubiquitinated. COS7 cells expressing wild-type HA-GlyT2 or HA-S512R mutant were treated with MG132 (10 μM, 4 h), lysed, and immunoprecipitated (*IP*) with the anti-HA monoclonal antibody, and the proteins recovered were probed with an anti-ubiquitin (P4D1) and anti-HA antibody. *White arrow*, GlyT2 (mature); *white arrowhead*, GlyT2 (immature); *black arrowhead*, S512R. *Small arrow*, 60 kDa band (24). High order bands of GlyT2 and S512R are indicated by *white* and *black squares*. *Asterisk*, IgG heavy chain + protein G. Means ± S.E. are shown. *, $p < 0.05$; **, $p < 0.01$, with respect to wild-type GlyT2 (means ± S.E., Student's *t* test). *D*, S512R is more prone to degradation than the wild-type GlyT2. COS7 cells expressing wild-type GlyT2 or S512R mutant were treated with 25 μM cycloheximide to block protein synthesis, and the transporter was monitored by immunoblotting of cell lysates with an anti-GlyT2 antibody at 0, 2, 6, and 24 h. Representative immunoblots (*WB*; *top panels*) and their densitometry (*bottom panels*) are shown. Tubulin immunoreactivity is shown as a loading control (means ± S.E. are shown). *PNGase F*, peptide:*N*-glycosidase F.

band was resistant to endoglycosidase H, indicating that it contained complex oligosaccharides, which would be consistent with a protein that has exited the ER, undergone oligosaccharide processing in the Golgi, and reached the cell surface. By contrast, the immature 75 kDa band was sensitive to Endo-H, indicating that it contained high mannose oligosaccharides borne by proteins in the ER. The glycosidase sensitivity of the S512R mutant paralleled that of the wild-type immature 75 kDa band, indicating that the mutant transporter resides in the ER.

The persistence of the S512R mutant in the ER suggests that this transporter is misfolded. Proteins that are folded incorrectly and are retained in the ER may be sorted for ER-associated degradation (ERAD) (38). Because most ERAD substrates are ubiquitinated by polychain addition prior to their degradation, we assessed the ubiquitination state of the wild-type and mutant transporters. As such, the HA-GlyT2 or HA-mutant transporter (see Fig. 5*A*) was immunoprecipitated from transfected COS7 cells with an anti-HA antibody, and the proteins recovered were analyzed in Western blots probed with an anti-ubiquitin (P4D1) antibody (Fig. 2*C*). Because ubiquitination regulates the endocytosis, recycling, and turnover of the mature GlyT2 (31, 37), it was not surprising that the 100 kDa band detected in the wild-type lysate was strongly ubiquitinated. Nevertheless, the ratio of ubiquitin to HA immunoreactivity was higher for the S512R mutant than the wild type (1.0 ± 0.23 *versus* 1.6 ± 0.19%), suggesting that S512R is modified by ubiquitination to a higher extent than the wild-type GlyT2. This was confirmed by immunoprecipitating the transporter with a KF2 multiubiquitin antibody (data not shown). In agreement with this, the S512R mutant was more prone to degradation. Cells expressing the wild-type or mutant transporter were treated with cycloheximide to block further protein synthesis, and a time course of transporter expression was monitored by immunoblotting at serial time intervals (Fig. 2*D*). Although mature

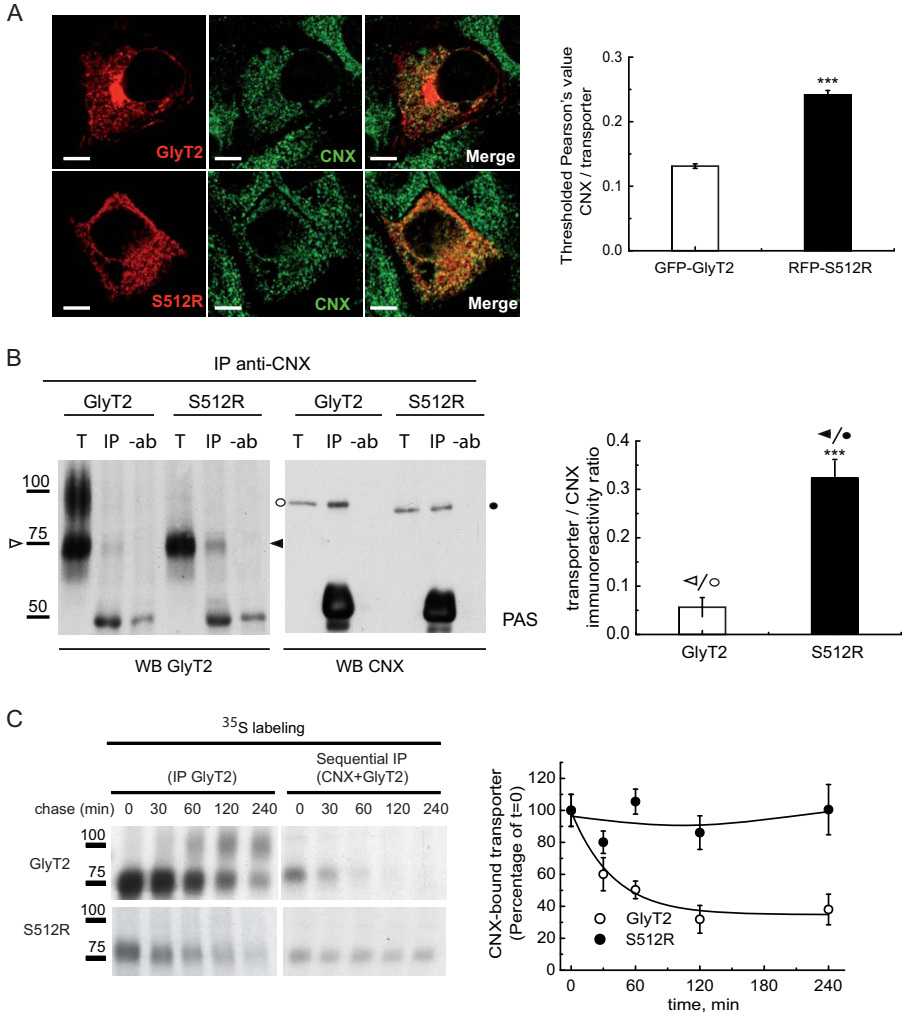

FIGURE 3. **Enhanced association of S512R with calnexin.** *A*, MDCK cells expressing either GFP-GlyT2 or RFP-S512R were immunolabeled for the ER chaperone CNX. For clarity, transporters are shown in *red*, and CNX is shown in *green* rather than in the original colors. Shown is quantification of the co-localization between GFP-GlyT2 and CNX or between RFP-S512R and CNX using Pearson's value of correlation as described under "Experimental Procedures": ***, $p < 0.001$ (Student's *t* test compared with GFP-GlyT2/CNX). *B*, immunoprecipitation of lysates from COS7 cells expressing either untagged GlyT2 or untagged S512R with the anti-CNX antibody. Immunocomplexes were probed in Western blots for GlyT2 (*left*) and CNX (*right*). *T*, total protein (input); *IP*, immunoprecipitated material; −*ab*, control without antibody. 75 kDa (ER) bands are indicated with *arrowheads* (*white*, GlyT2; *black*, S512R), and CNX (97 kDa) is indicated with *circles* (*white* or *black* in cells expressing GlyT2 or S512R). The GlyT2/CNX and S512R/CNX ratios in the immunoprecipitated material were calculated after densitometry of the bands indicated. ***, $p < 0.001$ (Student's *t* test compared with GlyT2/CNX). *C*, COS7 cells expressing the wild-type GlyT2 or S512R were pulse-labeled for 15 min with [^{35}S]methionine/cysteine and chased for the times indicated. The cell lysates were immunoprecipitated with the GlyT2 antibody (*left blot*) or subjected to sequential immunoprecipitation, first with CNX and then with the GlyT2 antibody (*right blot*), as described under "Experimental Procedures." *Right graph*, quantification of the transporter bound to CNX after densitometry of the fluorograms. The CNX-bound transporter was normalized to the total synthesized transporter at each time point and presented as a percentage of $t = 0$ taken as 100% (means ± S.E. (*error bars*) are shown). *WB*, Western blot.

wild-type GlyT2 had a half-life above 20 h (24), the amount of the mutant transporter was reduced by 50% within 2 h (49.7 ± 6.3%). Interestingly, the disappearance of the immature 75-kDa wild-type GlyT2 was faster than that of S512R, suggesting that maturation of GlyT2 was quicker than degradation of S512R. Thus, these results suggest that the S512R mutant is more prone to ERAD than wild-type GlyT2.

The Association of S512R with Calnexin Is Enhanced—The ER is a site where quality control of the glycoproteins synthesized takes place. Elements in the ER, such as molecular chaperones and lectins, recognize folding intermediates and undergo rounds of binding and release to facilitate or rescue folding, suppress aggregation, or mediate the retention and subsequent degradation of aberrant proteins. We recently showed that CNX plays an important role in the quality control of GlyT2 in the ER. The 75-kDa GlyT2 precursor transiently binds to CNX, which facilitates GlyT2 processing (24), and thus, the retention of the mutant in the ER may possibly reflect a more robust or long lasting association with CNX. Therefore, we studied the association of this chaperone to the wild-type or mutant transporter by confocal microscopy. In MDCK cells expressing either GFP-GlyT2 or RFP-S512R and immunostained for CNX, S512R co-localized more strongly with CNX than the wild-type GlyT2, as evident through the almost 2-fold increase in the Pearson value for the mutant (0.24 ± 0.006 *versus* 0.13 ± 0.003; Fig. 3*A*). Although these data suggest enhanced association to CNX of the mutant, the presence of mature and immature transporter forms in the wild type may make it difficult to compare with the co-localized fluorescence of the single-form mutant. Therefore, we assessed the amount

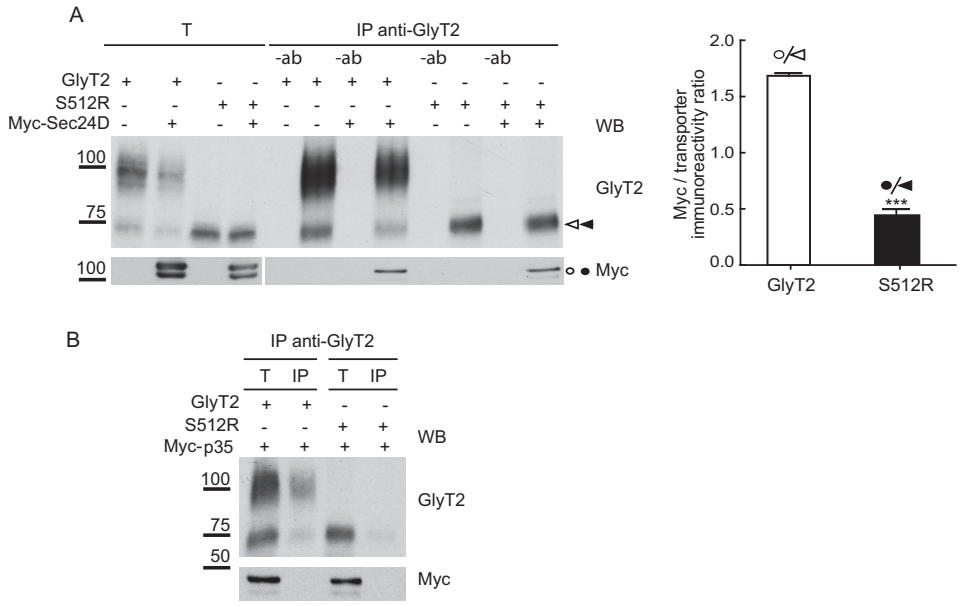

FIGURE 4. **The association of S512R with Sec24D is altered.** Lysates of COS7 cells expressing untagged GlyT2 or S512R in the presence or absence of Myc-Sec24D (A) or Myc-p35 (B) were immunoprecipitated with an anti-GlyT2 antibody, and the immunocomplexes were analyzed in Western blots to detect GlyT2 and Myc. *T*, total protein (input); *IP*, immunoprecipitated material; −*ab*, control without antibody. *Histogram*, Myc-Sec24D/GlyT2 and Myc-Sec24D/S512R ratios were calculated from the densitometry of the Myc bands (*circles*) and ER bands (*arrowheads*; GlyT2 (*white*) and S512R (*black*)): ***, $p < 0.001$ (Student's *t* test compared with Myc-Sec24D/GlyT2). *WB*, Western blot.

of untagged wild-type or mutant transporter recovered when Nonidet P-40 lysates of cells expressing these constructs were immunoprecipitated with an antibody against CNX. The amount of S512R co-precipitated from cells expressing this mutant with the CNX-specific antibody was 6-fold (6.4 ± 0.07) higher than the GlyT2 recovered from cells expressing the wild-type (Fig. 3*B*). This difference in steady-state binding might reflect a stronger or longer lasting association of the mutant transporter with CNX. To assess this possibility, sequential immunoprecipitation of [^{35}S]methionine/cysteine pulse-chased cells expressing the wild-type or mutant transporter was performed, whereby cell lysates were first immunoprecipitated with a CNX-specific antibody after a 15-min labeling pulse and the desired chase, and the immunocomplexes recovered were then immunoprecipitated with a GlyT2 antibody (Fig. 3*C*). In this way, a fraction of the protein bound to CNX in steady state could be isolated, and when the immunoprecipitation was performed after longer chases, we could estimate the half-life of the CNX-transporter complexes. Accordingly, the wild-type GlyT2 75-kDa precursor transiently associated with CNX in a complex with a half-life of around 60 min, at which point the 100-kDa mature transporter was formed (24). By contrast, the complex in which the mutant associated with CNX was much more stable (*right graph*), and this persistent association with CNX might lead to its retention in the ER.

Alterations in the Association of S512R with Sec24D—Cargo transport from the ER to the Golgi is mediated by COPII vesicles that bud off from the ER exit sites. ER export signals are thought to be recognized by the Sec24 subunit of the Sec24-Sec23 protein complex that forms the inner layer of the COPII coat. A binding site for Sec24 resides in the C terminus of several SLC6 transporters, which mostly depend on the Sec24D isoform for ER export (26, 32, 39). One possibility that could explain the slow dissociation of S512R from CNX is a distorted interaction of the mutant with the COPII, such that the delivery from the chaperone is impaired. To test this possibility, we expressed Myc-Sec24D protein in COS7 cells together with either the wild-type GlyT2 or S512R transporter, immunoprecipitated the cell lysates with a GlyT2-specific antibody, and probed the immunocomplexes in Western blots to detect Myc-Sec24D. The amount of Myc-Sec24D co-immunoprecipitated with the 75-kDa wild-type GlyT2 was 4-fold (4.3 ± 0.12) higher than that recovered with the mutant (Fig. 4*A*). This interaction was independent of the Myc tag because a Myc-tagged negative control did not interact with the transporters (Fig. 4*B*). This suggests that the binding of the mutant to Sec24D is somehow altered, and as a consequence, S512R is not exported from the ER.

S512R Forms Oligomers with Wild-type GlyT2—Upon release of the lumenal ER chaperones, most exportable proteins oligomerize, which helps to relieve ER entrapment. However, by forming heteromers with the S512R mutant, it is possible that the wild type could be retained in the ER. To test this hypothesis, we immunoprecipitated lysates of cells expressing differently tagged wild-type and mutant transporters (HA or RFP N-terminal fusions of the transporters that do not interfere with expression or function; Fig. 5*A*), and using a specific antibody against one tag, we monitored the co-precipitation of the other transporter by Western blot. Due to the small size of the HA epitope (less than 1 kDa), the HA-tagged transporters were virtually indistinguishable from the untagged counterparts, so that HA-GlyT2 showed the two bands of about 100 and 75 kDa, and HA-S512R showed the 75 kDa band. By contrast, the pRFP vector used contained a tandem dimer variant of DsRed (27) that increased the size of the bands by ~75 kDa, such that RFP-S512R appeared as a 150 kDa band, and RFP-GlyT2 appeared as a doublet of 175 and 150 kDa. Some additional bands were also observed due to the tendency of the untagged

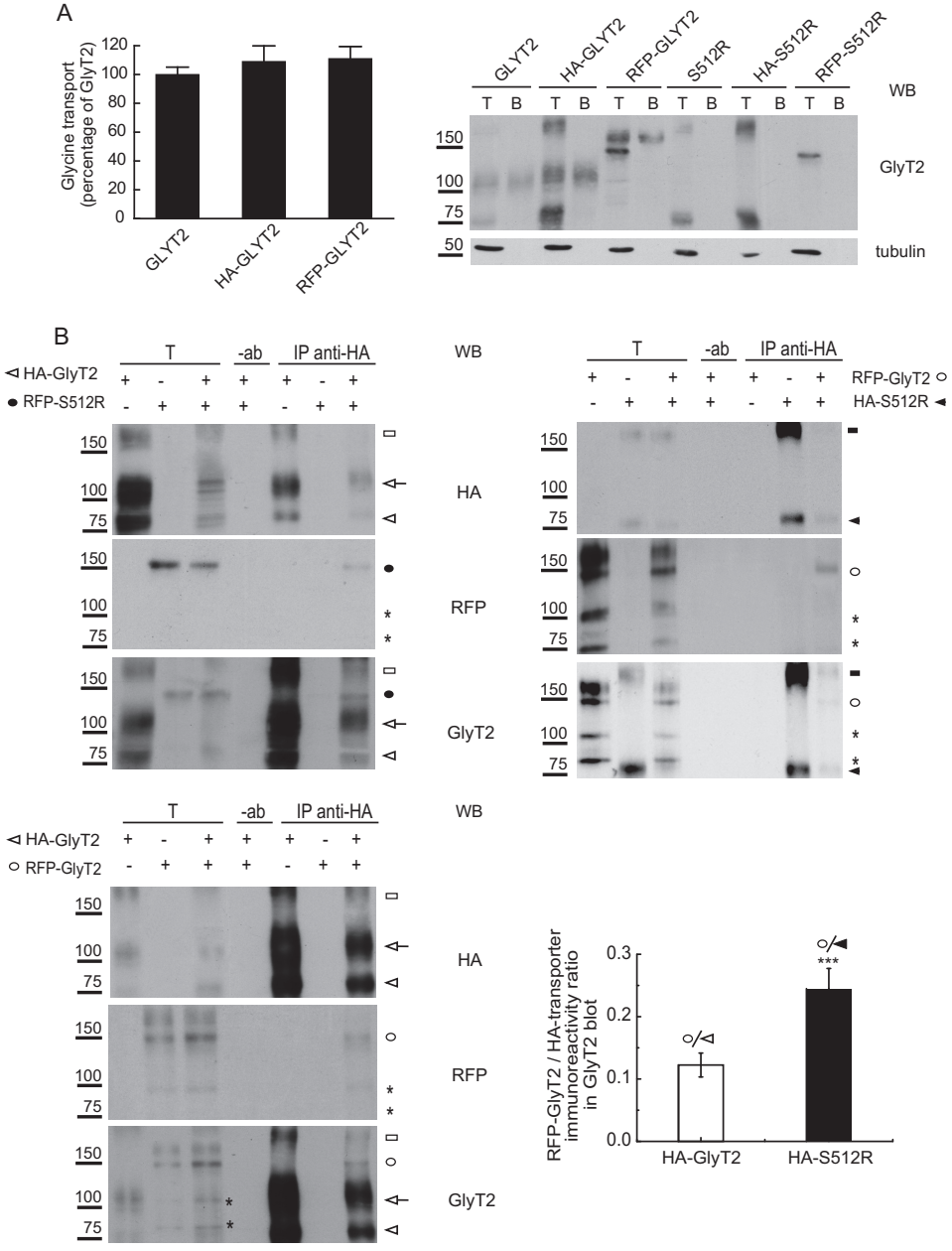

FIGURE 5. **S512R co-immunoprecipitates with wild-type GlyT2.** *A*, glycine transport and surface biotinylation was measured in COS7 cells expressing the indicated untagged or tagged transporters, as described under "Experimental Procedures," and the 100% untagged wild-type GlyT2 transport was 2.8 ± 0.5 nmol/mg protein/10 min (mean ± S.E. (*error bars*)). *T*, total transporter; *B*, biotinylated transporter. *B* and *C*, S512R co-immunoprecipitates with wild-type GlyT2. Lysates of COS7 cells expressing the indicated tagged transporters were immunoprecipitated with anti-HA antibody, and the immunocomplexes were analyzed in Western blots to detect HA, RFP, and GlyT2. *T*, total protein (input); *IP*, immunoprecipitated material; −*ab*, control without antibody. Transporter proteins are indicated as follows. *White arrowhead*, HA-GlyT2 (immature); *white arrow*, HA-GlyT2 (mature); *black circle*, RFP-S512R; *white circle*, RFP-GlyT2 (immature); *black arrowhead*, HA-S512R. High order bands of GlyT2 and S512R are indicated with *white* and *black squares*. *Asterisks* indicate small proteolytic fragments. *Histogram*, the RFP-GlyT2/HA-GlyT2 and RFP-GlyT2/HA-S512R ratios were calculated by densitometry of the indicated ER bands of GlyT2 Western blots (the means ± S.E. are shown): ***, $p < 0.001$ (Student's *t* test compared with HA-GlyT2/CNX). *WB*, Western blot.

or tagged 75-kDa form to generate higher molecular weight forms, clearly recognizable in the GlyT2 Western blots. Also, some small proteolytic products were observed, such as two bands slightly above 100 and 75 kDa. When the anti-HA antibody was used to immunoprecipitate the transporter from cells expressing HA-GlyT2 and RFP-S512R, alone and in combination (a condition that gave clean Western blots when probed for HA, RFP, or GlyT2; Fig. 5*B*, *left*), both tagged proteins were present in the HA immunoprecipitate, indicating that the wild type and mutant interact. This interaction was also detected when we exchanged the tags and co-expressed HA-S512R with RFP-GlyT2 and probed Western blots of the immunocomplexes obtained with anti-HA for RFP-GlyT2 (Fig. 5*B*, *right*). Notably, the 150 kDa RFP-tagged band was that primarily recovered from these cells, suggesting that the wild-type-mutant interaction mainly involves the 75-kDa ER wild-type form. A similar result was obtained when HA was used to immunoprecipitate complexes from cells co-expressing HA-GlyT2 and RFP-GlyT2, indicating that also for the wild-type, the immature forms do interact. The amount of RFP-GlyT2 co-immunopre-

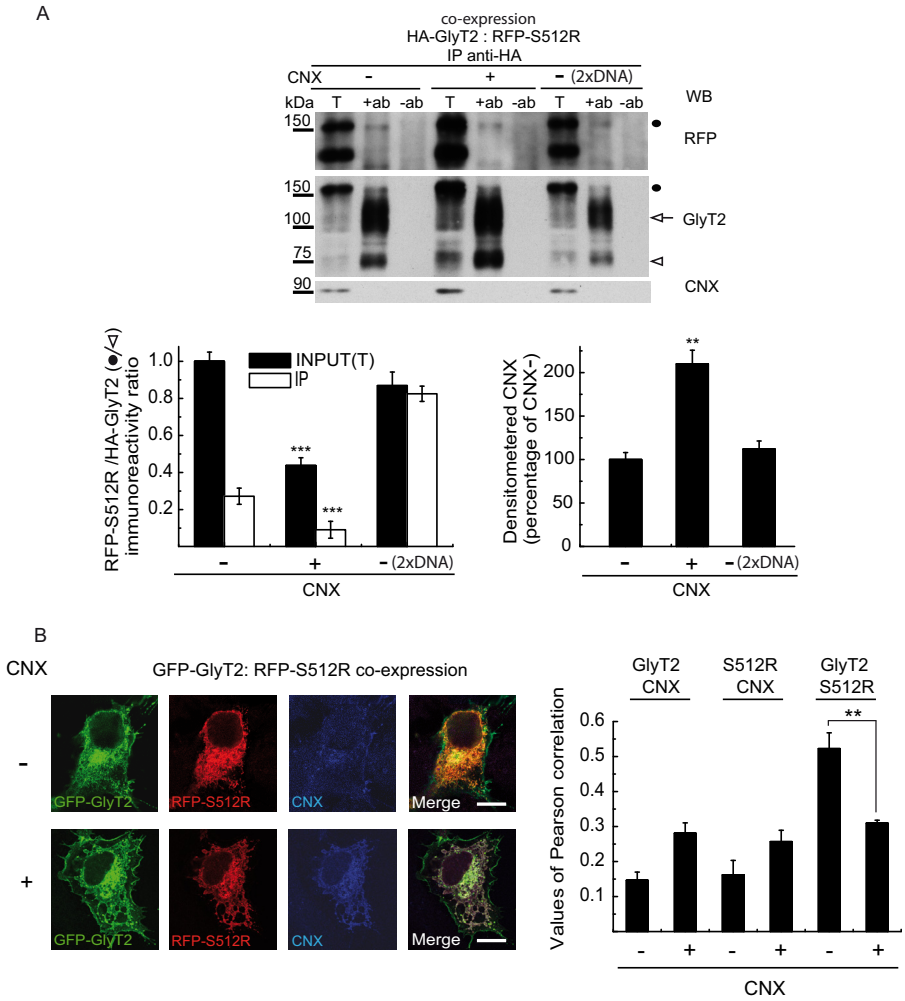

FIGURE 6. **Effect of CNX overexpression on GlyT2-S512R interaction.** *A*, Western blot (*WB*) probed for GlyT2, RFP, and CNX of immunocomplexes obtained with an HA antibody from cells co-expressing HA-GlyT2 and RFP-S512R in the presence or absence of overexpressed recombinant CNX (1:4 cDNA ratio). The control (2× DNA) corresponds to COS7 cells transfected with double the concentration of HA-GlyT2 and RFP-S512R cDNAs. *T*, total protein (input); *IP*, immunoprecipitated material; *−ab*, control without antibody. *Black circle*, RFP-S512R; *white arrow* and *arrowhead*, HA-GlyT2 100 and 75 kDa bands, respectively. The RFP-S512R/HA-GlyT2 immunoreactivity ratios (*left*) and CNX immunoreactivity (*right*) were calculated by densitometry of the corresponding bands: **, $p < 0.01$; ***, $p < 0.001$ (ANOVA with Tukey's post hoc test compared with controls without overexpressed calnexin: *CNX −*). *B*, MDCK cells expressing GFP-GlyT2 and RFP-S512R in the presence (*CNX+*) or absence (*CNX−*) of overexpressed CNX were immunolabeled for CNX. Shown is quantification of the co-localization between GFP-GlyT2/CNX, RFP-S512R/CNX, or GFP-GlyT2/RFP-S512R in the presence (*CNX+*) or absence (*CNX−*) of exogenous CNX, using Pearson's value of correlation as described under "Experimental Procedures" (means ± S.E. (*error bars*) are shown): **, $p < 0.01$ (Student's *t* test compared with control without overexpressed CNX; *CNX−*).

cipitated with HA-S512R was 2-fold (2.0 ± 0.45) higher than that co-immunoprecipitated with HA-GlyT2, suggesting a stronger association of the wild type with the mutant than with other wild-type molecules (Fig. 5*C*, *right histogram*).

CNX Overexpression Rescues Wild-type GlyT2 from the Dominant Negative Effect of S512R—Because the S512R mutant showed enhanced association to CNX (Fig. 3) and it also interacts with wild-type GlyT2 (Fig. 5), we asked whether overexpressing CNX might affect the interaction between the wild-type and mutant transporter. Recombinant CNX was overexpressed in cells co-expressing HA-GlyT2 and RFP-S512R, and the amount of the RFP-mutant transporter co-precipitated with HA-GlyT2 from the cell lysates was quantified by densitometry in Western blots probed for RFP-S512R (Fig. 6*A*). CNX overexpression preferentially favored the accumulation of wild-type GlyT2 in the cells and significantly reduced the mutant/wild-type ratio in the immunocomplexes (*bottom left histogram*). In addition, total transporter expression was increased by the chaperone, consistent with our previous results showing that CNX facilitated GlyT2 biogenesis (24). However, the weaker contribution of RFP-S512R to the complexes was not due to a general increase in transporter expression because enhancing transporter expression by doubling the amount of transporter cDNA used in the transfection did not alter mutant and wild-type co-immunoprecipitation. This was due to the fact that overexpressed CNX increased wild-type transporter expression to a greater extent than mutant expression, which probably reflects the chaperone's ability to discriminate between different conformational states of GlyT2 (24). The overexpression of CNX in COS7 cells co-expressing GFP-GlyT2 and RFP-S512R also provoked a significant decrease in the co-localization of wild-type and mutant immunofluorescence, reflected in the drop in the Pearson value to 59.09 ± 0.12% of its value at endogenous CNX levels (0.44 ± 0.09 *versus*

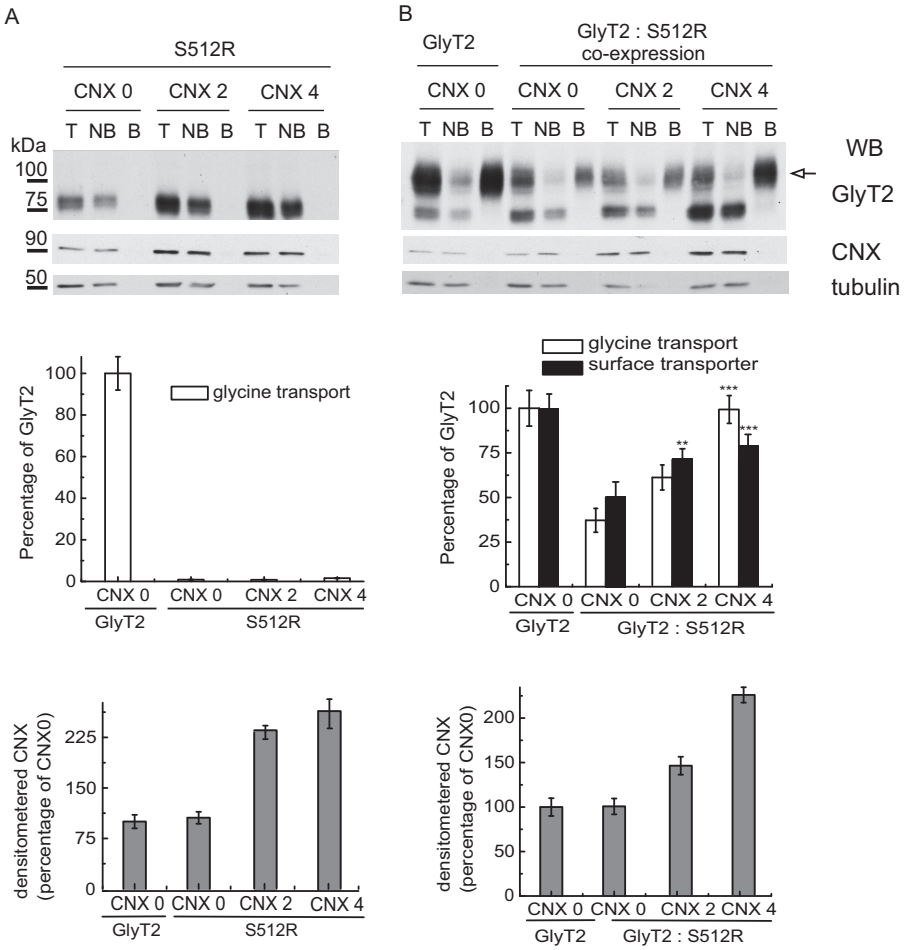

FIGURE 7. **CNX overexpression rescues the function and membrane expression of the wild-type transporter from the dominant negative effect of S512R.** Biotinylation and glycine transport of COS7 cells transfected with untagged S512R cDNA (*A*) or untagged wild-type GlyT2 cDNA, alone or in combination at a 1:1 ratio by weight (*B*), together with increasing concentrations of exogenous CNX cDNA (*0*, *2*, and *4* refer to a 1:0, 1:2, and 1:4 GlyT2/CNX cDNA ratio by weight). *Top panels*, Western blots (*WB*) of streptavidin agarose-bound transporters. *T*, total transporter; *B*, biotinylated transporter; *NB*, non-biotinylated transporter. Biotinylated bands were quantified by densitometry. Tubulin is shown as a non-biotinylated protein control. Surface GlyT2 (100 kDa band, *arrow*) expression is represented in the *middle panel* as *black bars* together with glycine transport (*white bars*). 100% glycine transport was 2.8 ± 0.3 nmol/mg of protein/10 min (mean ± S.E. (*error bars*)). Western blot membranes were reprobed for CNX to verify overexpression, and the CNX bands quantified and normalized to tubulin are shown in the *lower graphs* in *A* and *B*: **, $p < 0.01$; ***, $p < 0.001$ (ANOVA with Tukey's post-hoc test compared with the control with no overexpressed CNX: *CNX 0*).

0.26 ± 0.03; Fig. 6*B*). Remarkably, when the wild-type and mutant transporters were co-expressed, the stronger co-localization of S512R/CNX relative to wild type/CNX that was observed when the transporters were expressed alone with CNX (Fig. 3) was barely or not evident (see "Discussion").

To determine whether CNX overexpression could rescue the function of wild-type GlyT2 from the dominant negative effect of S512R, untagged transporters were expressed alone or together at a 1:1 ratio (which we expect to mimic heterozygosis) in the presence of increasing concentrations of CNX, assessing membrane expression and glycine transport in these cells (Fig. 7). The amount of CNX was monitored by densitometry and normalized to tubulin immunoreactivity (*bottom histograms*). The capacity of the S512R mutant to form a functional transporter with mature glycosylation could not be rescued by CNX despite a 3-fold increase in the amount of 75-kDa S512R that was detected. By contrast, an increase in the concentration of CNX produced partial rescue of the function and membrane expression of wild-type GlyT2 when it was co-transfected with S512R (*right panels*). Interestingly, the recovery of transporter activity was slightly higher than the enhancement of membrane expression, suggesting either more efficient folding of the membrane transporter in the presence of the chaperone (24) or a CNX-induced stimulation of transport activity of unknown nature.

Rescue of Wild-type GlyT2 from the Dominant Negative Effect of the S512R Mutant by Chemical Chaperones—The previous results suggest that treatments increasing the expression or accelerating the processing and membrane translocation of GlyT2 could rescue the dominant negative effect produced by S512R. Folding mutants of some membrane proteins, such as ATP-binding cassette transporters, can be corrected with ligands/substrates (40, 41). Although the pharmacology of GlyT2 is very scarce, we incubated transfected COS7 cells during the protein processing of this transporter (48 h post-transfection) with several glycine analogues known to inhibit GlyT2 transport to some extent (42). Only glycine produced some rescue (27.3 ± 5.1% of transport and 10.1 ± 2.6% of mature transporter; Fig. 8*A*), although a minor effect was also detected with glycine methyl ester. Conversely, neither the specific GlyT2

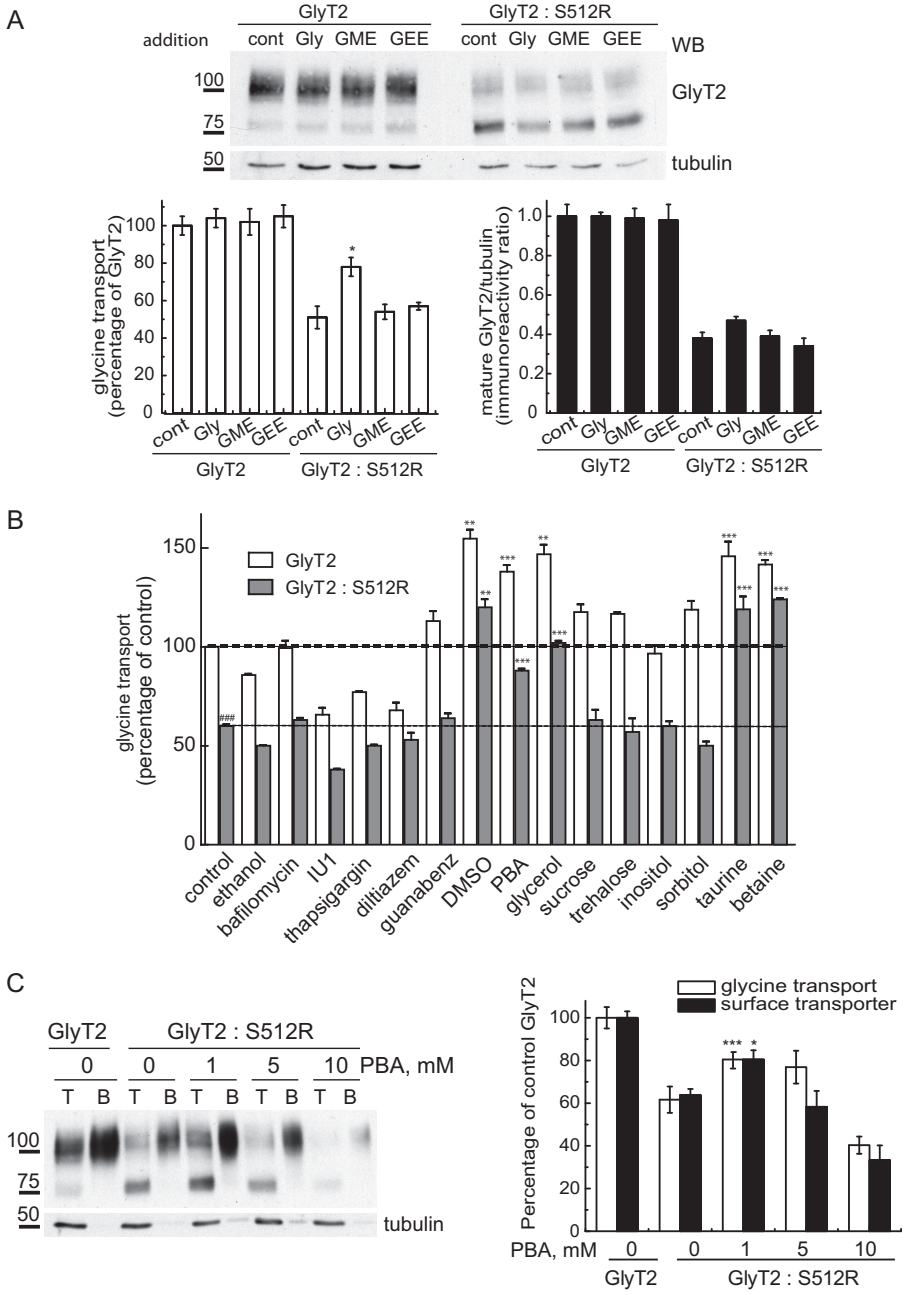

FIGURE 8. **Chemical chaperones rescue the wild-type transporter from the dominant negative effect of S512R.** *A*, COS7 cells expressing wild-type GlyT2 alone or co-expressed with S512R in a 1:1 ratio were incubated for 72 h (before and during transporter biogenesis) with 5 mM glycine (*Gly*), glycine methyl ester (*GME*), or glycine ethyl ester (*GEE*), and 48 h post-transfection, they were analyzed in Western blots (*WB*) and for glycine transport. *Top*, Western blots probed for GlyT2 and tubulin as a loading control. *Bottom right*, densitometry of the 100-kDa mature GlyT2 band normalized to tubulin immunoreactivity. *Bottom left*, glycine transport relative to the control GlyT2 (alone), 100% glycine transport 2.7 ± 0.4 nmol/mg of protein/10 min (mean ± S.E. (*error bars*)): ###, $p < 0.001$ (Student's *t* test compared with GlyT2 alone); **, $p < 0.01$; ***, $p < 0.001$ (ANOVA with Tukey's post hoc test compared with control GlyT2/S512R). *B*, conditions identical to those in *A*, except the cells were incubated with 200 nM bafilomycin, 50 μM IU1, 1 μM thapsigargin dissolved in ethanol (vehicle), 20 μM diltiazem, 5 mM guanabenz, 1% DMSO, 1 mM PBA, 1% glycerol, 100 mM sucrose, trehalose, inositol, sorbitol, taurine, and betaine. *C*, conditions identical to those in *A*, except the cells were incubated with increasing concentrations of PBA and subjected to surface biotinylation. *Left*, Western blot after biotinylation; *right*, glycine transport (relative to GlyT2 alone: 2.1 ± 0.3 nmol/mg of protein/10 min, mean ± S.E.) and surface GlyT2 densitometry (means ± S.E.).

inhibitor ALX1393 nor sarcosine, a GlyT1-specific substrate, could provoke significant rescue (data not shown). We next assessed general chemical chaperones, drugs that can aid the folding of membrane proteins and accelerate their trafficking to the membrane. These compounds belong to three main classes of osmolytes (43): carbohydrates (glycerol, sorbitol, and inositol); amino acids and derivatives (glycine, taurine, alanine, and proline); and methylamines (betaine and trimethylamine *N*-oxide). Hence, we tested several representatives of each class, together with substances that influence cell proteostasis and other more generally accepted chemical chaperones: sodium 4-phenylbutyrate (PBA) (44) and the autophagy inducer trehalose (45). Like CNX, no compound produced any effect on S512R expressed alone; however, the transport activity of wild-type GlyT2 when expressed alone or together with S512R was significantly stimulated (increases of 40–60%) by dimethyl

sulfoxide (DMSO), PBA, glycerol, taurine, and betaine. Thus, the wild-type GlyT2 was rescued from the dominant negative effect of S512R (Fig. 8*B*). Of these compounds, DMSO and glycerol produced some toxicity on the cells (not shown), whereas taurine and betaine were effective at very high concentrations (100 mM). By contrast, the maximal effect of PBA was observed at 1 mM, and it produced an increase in glycine transport (40.6 ± 9.6%, mean ± S.E.) and membrane expression of the active transporter (38.1 ± 9.5%, mean ± S.E.) comparable with CNX (Fig. 8*C*). In addition, no toxic effects on COS7 cells were detected, as would be expected for a compound approved by the United States Food and Drug Administration for use in humans (46).

In light of these data, we assayed this compound in primary cortical neurons, which displayed robust surface co-localization of two differentially tagged wild-type transporters (GFP-GlyT2 and RFP-GlyT2). However, GFP-GlyT2 and RFP-S512 co-expression in these cells reproduced the dominant negative effect observed in non-neural cells, with strong intracellular staining of both transporters and reduced surface expression of the wild-type GlyT2 (Fig. 9*A*). Indeed, when the dominant negative effect detected in neurons was quantified, it was comparable with that observed in COS7 cells (Fig. 9*B*). It is noteworthy that the size of the immature and mature GlyT2 was barely distinguishable in Western blots of neurons, probably due to neuron-specific patterns of glycosylation.[4] Nevertheless, the expression was strong enough to measure robust transport activity in the presence of the GlyT1 inhibitor NFPS (about 5 and 1.3 nmol of glycine/mg of protein/7 min in GlyT2 and mock-transfected neurons, respectively). The expression of the wild-type and mutant transporters at a 1:1 ratio reduced GlyT2 membrane expression to 34.1 ± 5.3 and glycine transport to 42.5 ± 4.1% (mean ± S.E.). Moreover, a further increase in the concentration of the co-expressed mutant provoked an additional decrease in transporter expression and function. Remarkably, PBA (1 mM) promoted significant rescue of this effect and restored both membrane expression (92.6 ± 8.6%) and glycine transport (86.1 ± 8.4%) of the active GlyT2 co-expressed with the mutant in these primary neurons. Thus, for the first time, our results show the possibility of overcoming the dominant negative effect of the S512R mutant in a neuronal preparation.

DISCUSSION

In this report, we have verified and characterized the dominant negative effect of the S512R mutant of GlyT2, whose co-expression with the wild-type transporter provokes a considerable reduction in glycine transport and prevents it from reaching the plasma membrane, both in COS7 cells and in primary cortical neurons.

S512R is a folding-defective mutant that does not produce a mature transporter; rather, the immature transporter is retained in the ER. Its apparent molecular weight and glycosidase sensitivity indicates its processing is arrested after receiving the first preassembled glycans, transferred by the oligosaccharyltransferase to the Asn-*X*-Ser/Thr consensus sites from the lipid dolichol-pyrophosphate donor in the ER membrane. The glycans are then rapidly trimmed in a co-translational manner by the sequential action of glucosidases I and II to generate monoglucosylated side chains that support binding to lectin chaperones like CNX (47). For this reason, S512R is a preferred substrate for CNX, and its association with the chaperone is stronger than that of the wild-type transporter, as witnessed by co-immunoprecipitation and fluorescence co-immunolocalization. This association provokes the ER retention of the mutant transporter. Retention of misfolded proteins in the ER leads to their polychain ubiquitination, a signal for degradation by the 26 S proteasome through ERAD. Our results indicate that CNX-retained S512R is targeted for ERAD because it is more intensely ubiquitinated than the wild-type GlyT2 and it has a much shorter half-life. The fact that CNX overexpression cannot rescue the mutant indicates that chaperone binding precedes degradation and not maturation, as occurs in the wild type.

Misfolding of S512R seems to be due to the introduction of the large positive charged arginine rather than the removal of the serine. Two additional hyperekplexia-associated missense mutations have been identified in the same TM7 region, both predicting clashes or disturbances of crucial residues involved in Na1 and Cl^- coordination (N511S and S515I, rat position numbering) (10, 12). Hence, substitutions in this important region alter the protein's function, although only severe structural alterations may provoke its misfolding. This suggests that Ser-512, which is located at the membrane-exposed surface of the transporter, may expose motifs (hydrophobic patches or unpaired cysteines) involved in chaperone binding when replaced by arginine. In the recently modeled *Drosophila* DAT, the serine homologous to Ser-512 is situated in a groove between TM5 and TM7, where a cholesterol molecule is bound to the transporter. Therefore, Ser-512, although not directly involved in the binding of cholesterol, is shielded by the bound cholesterol molecule, and it may influence the binding site. A modulatory role in maintaining an outward-open state of the transporter has been proposed for the cholesterol-binding site (19). As in DAT, the GlyT2 transport is modulated by cholesterol, and the transporter displays optimal transport activity when included in lipid rafts (31). The modulation of transport by cholesterol suggests a connection between the cholesterol binding site and the substrate binding site. New data from the DAT crystal suggested that the bound cholesterol molecule modulates the movement of TM1a that occurs during the transport cycle. TM1a is connected to internal loop 1, which in turn is hydrogen-bonded to the C-terminal latch of the transporter. In several SLC6 members, this region contains the binding site for the cargo receptor of the COPII complex Sec24 that permits ER export (26, 39), and C-terminal deletion mutants of GlyT2 are retained in the ER (32). We have demonstrated that the interaction of wild-type GlyT2 with Sec24D is altered in the S512R mutant. Although this alteration has to be confirmed with endogenous Sec24D in neural preparations, we hypothesize that the S512R mutation causes structural distortion of the cholesterol modulatory region that is transmitted to the C-terminal latch and that somehow influences the interaction with

[4] E. Arribas-González, J. de Juan-Sanz, C. Aragón, and B. López-Corcuera, unpublished results.

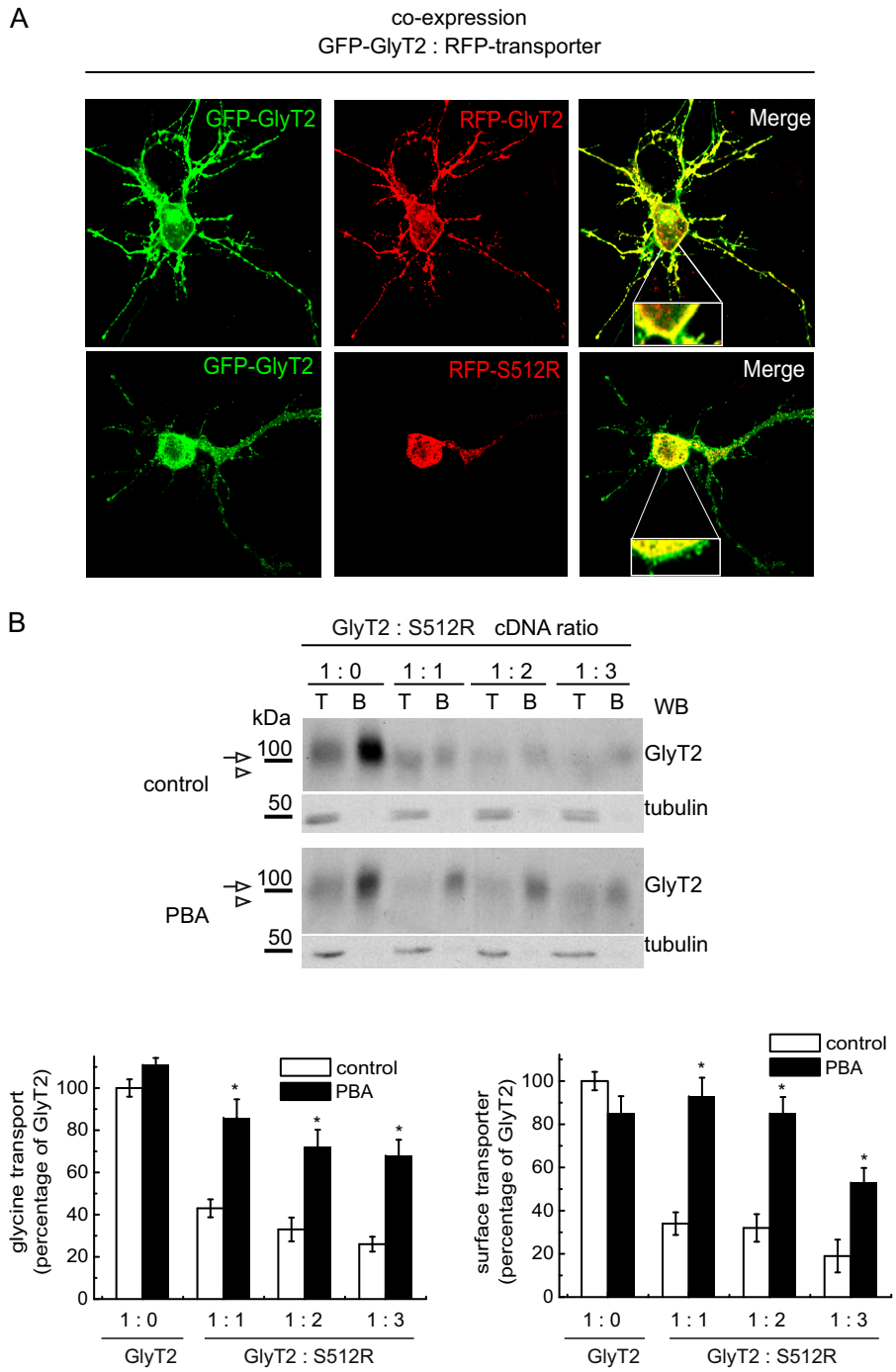

FIGURE 9. **PBA rescues the wild-type transporter from the dominant negative effect of S512R in primary neurons.** *A*, confocal microscopy images of cortical neurons co-expressing the indicated tagged transporters. GFP-GlyT2 or RFP transporters were detected with the corresponding anti-tag antibody and are shown in *green* or *red*, respectively. *B*, cortical neurons maintained *in vitro* for 7 days were transfected with wild-type GlyT2 cDNA alone or with increasing amounts of S512R cDNA to reach the indicated GlyT2/S512R cDNA ratios (by weight). The cells were treated 4 h post-transfection with 1 mM PBA or with the vehicle alone (Neurobasal/B27 culture medium) and subjected to biotinylation and glycine transport determination. *Top*, Western blot after biotinylation. Mature GlyT2 bands are indicated with an *arrow*. An *arrowhead* indicates the position of the immature transporter. *T*, total transporter; *B*, biotinylated transporter. Tubulin immunoreactivity is shown as a non-biotinylated protein control. Bands were quantified by densitometry, and biotinylated GlyT2 is represented in the *right histogram*. *Left histogram*, glycine transport relative to GlyT2 alone (100% glycine transport, 3.2 ± 0.5 nmol/mg protein/10 min; mean ± S.E.): *, $p < 0.05$ (ANOVA with Tukey's post hoc test compared with the absence of PBA). *WB*, Western blot.

COPII to provoke its retention in the ER. It is tempting to speculate that cholesterol binding to the mutant might be impaired, although this could not be proven in our hands due to the effects of altering cholesterol concentrations on the proteostasis of the cells (data not shown) (50).

In this study, we have also shown that wild-type GlyT2 forms oligomers with the S512R mutant and that this interaction is more stable than its binding to other wild-type molecules. This interaction mainly takes place in the ER, such that ER retention of the wild-type/mutant oligomers prevents the progression of

GlyT2 through the secretory pathway and explains the dominant negative behavior of the mutant. CNX overexpression rescues this effect, suggesting that the wild-type and mutant isoforms compete for binding to the chaperone, which may facilitate the selective transport of the wild-type folded transporter to the plasma membrane (24). The fact that the association of S512R with the wild-type GlyT2 is diminished in the presence of overexpressed CNX, despite its more persistent binding to CNX and its enhanced association with the wild-type isoform, sustains the selective role of the chaperone. GlyT2 oligomerization was previously shown after transporter cross-linking (49). Our data confirm that oligomer formation is required for ER export, as demonstrated for other SLC6 transporters (26). Therefore, the immature GlyT2 forms appear to bind to CNX prior to the formation of oligomers, and they are subsequently exported from the ER to continue transporter maturation.

Chemical chaperones are non-selective small molecules that stabilize mutant proteins and accelerate their membrane trafficking, reminiscent of the chaperoning function of intracellular molecular chaperones (43). Due to this activity, chemical chaperones may potentially have therapeutic value to improve ER stress-related pathologies (41). Most chemical chaperones are osmotically active, such that they equilibrate cellular osmotic pressure during ER crowding. Here, the effect of chemical chaperones in the rescue of GlyT2 was analyzed in cultured cells and transfected cortical neurons. According to CNX action, no effect of any of these compounds was seen on S512R expressed alone. However, the influence of these molecules on the dominant negative effect of the mutant allows us to speculate on the conditions that might favor correct GlyT2 folding. The calcium concentration seems not to be critical for GlyT2 folding because no significant effect was observed in the presence of compounds that reduce (thapsigargin) or increase (diltiazem) ER calcium levels. Conversely, substantial rescue was detected with the antioxidant molecule DMSO, in agreement with the high number of cysteines present in GlyT2. The osmotically active compounds glycerol, taurine, and betaine promote significant rescue, suggesting that some ER crowding takes place. Moreover, although we found no protein kinase-like endoplasmic reticulum kinase phosphorylation, we did detect some increase in BiP expression (2.3 $\pm$ 0.4-fold), suggesting some enhancement of the unfolded protein response (50) when the mutant was expressed or co-expressed with the wild type. However, no effect was observed for activators of the proteasome (IU1) (44) or autophagy (trehalose) (45) or inhibitors of bulk aggregation (guanabenz) (44). Still, our data did indicate that PBA produces significant rescue in mild conditions that produce no toxic effects, both in COS7 cells and in cultured neurons. PBA increases GlyT2 transport activity and plasma membrane expression by fulfilling chaperone-like activity, as proven for other misfolded pathogenic proteins (44, 51). PBA is an interesting compound because not only is it a chemical chaperone approved by the Food and Drug Administration for use in humans, but it can also pass across the blood-brain barrier, and it has been implicated as a protective agent in neurodegenerative diseases involving ER stress (52). Therefore, PBA may potentially rescue the dominant negative effect of GlyT2 mutants inherited in heterozygosis, positively affecting glycinergic neural transmission by accelerating membrane trafficking of GlyT2. Our results support the possibility that selective pharmacoperones (17) that may enter cells and may bind specifically to misfolded mutant GlyT2, correct its folding, and allow correct routing have potential therapeutic effects in hyperekplexia. However, further work along these lines must be carried out to confirm this hypothesis.

Acknowledgments—We thank Francisco Zafra, Jose Antonio Esteban, José María Requena, and Pablo Alonso-Torres (Centro de Biología Molecular Severo Ochoa) for generously providing the Myc-Sec24D, Myc-p35, and HA-GlyT2 constructs in pcDNA3, the pRFP vector, the in-house RFP antibody, and S512R in pcDNA3, respectively. The expert technical assistance of Enrique Núñez is also acknowledged. We are grateful to the confocal microscopy facility at the Centro de Biología Molecular Severo Ochoa for valuable and expert help with the confocal microscopy work.

REFERENCES

1. Aragón, C., and López-Corcuera, B. (2003) Structure, function and regulation of glycine neurotransporters. *Eur. J. Pharmacol.* **479,** 249–262
2. Gomeza, J., Ohno, K., Hülsmann, S., Armsen, W., Eulenburg, V., Richter, D. W., Laube, B., and Betz, H. (2003) Deletion of the mouse glycine transporter 2 results in a hyperekplexia phenotype and postnatal lethality. *Neuron* **40,** 797–806
3. Aragón, C., and López-Corcuera, B. (2005) Glycine transporters: crucial roles of pharmacological interest revealed by gene deletion. *Trends Pharmacol. Sci.* **26,** 283–286
4. Rousseau, F., Aubrey, K. R., and Supplisson, S. (2008) The glycine transporter GlyT2 controls the dynamics of synaptic vesicle refilling in inhibitory spinal cord neurons. *J. Neurosci.* **28,** 9755–9768
5. Apostolides, P. F., and Trussell, L. O. (2013) Rapid, activity-independent turnover of vesicular transmitter content at a mixed glycine/GABA synapse. *J. Neurosci.* **33,** 4768–4781
6. Bakker, M. J., van Dijk, J. G., van den Maagdenberg, A. M., and Tijssen, M. A. (2006) Startle syndromes. *Lancet Neurol.* **5,** 513–524
7. Bakker, M. J., van Dijk, J. G., van den Maagdenberg, A. M., and Tijssen, M. A. (2006) Startle syndromes. *Lancet Neurol.* **5,** 513–524
8. Harvey, R. J., Topf, M., Harvey, K., and Rees, M. I. (2008) The genetics of hyperekplexia: more than startle!. *Trends Genet.* **24,** 439–447
9. Harvey, R. J., and Yee, B. K. (2013) Glycine transporters as novel therapeutic targets in schizophrenia, alcohol dependence and pain. *Nat. Rev. Drug Discov.* **12,** 866–885
10. Rees, M. I., Harvey, K., Pearce, B. R., Chung, S. K., Duguid, I. C., Thomas, P., Beatty, S., Graham, G. E., Armstrong, L., Shiang, R., Abbott, K. J., Zuberi, S. M., Stephenson, J. B., Owen, M. J., Tijssen, M. A., van den Maagdenberg, A. M., Smart, T. G., Supplisson, S., and Harvey, R. J. (2006) Mutations in the gene encoding GlyT2 (SLC6A5) define a presynaptic component of human startle disease. *Nat. Genet.* **38,** 801–806
11. Eulenburg, V., Becker, K., Gomeza, J., Schmitt, B., Becker, C. M., and Betz, H. (2006) Mutations within the human GLYT2 (SLC6A5) gene associated with hyperekplexia. *Biochem. Biophys. Res. Commun.* **348,** 400–405
12. Carta, E., Chung, S. K., James, V. M., Robinson, A., Gill, J. L., Remy, N., Vanbellinghen, J. F., Drew, C. J., Cagdas, S., Cameron, D., Cowan, F. M., Del Toro, M., Graham, G. E., Manzur, A. Y., Masri, A., Rivera, S., Scalais, E., Shiang, R., Sinclair, K., Stuart, C. A., Tijssen, M. A., Wise, G., Zuberi, S. M., Harvey, K., Pearce, B. R., Topf, M., Thomas, R. H., Supplisson, S., Rees, M. I., and Harvey, R. J. (2012) Mutations in the GlyT2 gene (*SLC6A5*) are a second major cause of startle disease. *J. Biol. Chem.* **287,** 28975–28985
13. Giménez, C., Pérez-Siles, G., Martínez-Villarreal, J., Arribas-González, E., Jiménez, E., Núñez, E., de Juan-Sanz, J., Fernández-Sánchez, E., García-Tardón, N., Ibáñez, I., Romanelli, V., Nevado, J., James, V. M., Topf, M.,

Chung, S. K., Thomas, R. H., Desviat, L. R., Aragón, C., Zafra, F., Rees, M. I., Lapunzina, P., Harvey, R. J., and López-Corcuera, B. (2012) A novel dominant hyperekplexia mutation Y705C alters trafficking and biochemical properties of the presynaptic glycine transporter GlyT2. *J. Biol. Chem.* **287,** 28986–29002
14. Kanner, B. I., and Zomot, E. (2008) Sodium-coupled neurotransmitter transporters. *Chem. Rev.* **108,** 1654–1668
15. Rudnick, G., Krämer, R., Blakely, R. D., Murphy, D. L., and Verrey, F. (2014) The SLC6 transporters: perspectives on structure, functions, regulation, and models for transporter dysfunction. *Pflugers Arch.* **466,** 25–42
16. Pérez-Siles, G., Núñez, E., Morreale, A., Jiménez, E., Leo-Macías, A., Pita, G., Cherubino, F., Sangaletti, R., Bossi, E., Ortíz, A. R., Aragón, C., and López-Corcuera, B. (2012) An aspartate residue in the external vestibule of GLYT2 (glycine transporter 2) controls cation access and transport coupling. *Biochem. J.* **442,** 323–334
17. Conn, P. M., and Janovick, J. A. (2009) Drug development and the cellular quality control system. *Trends Pharmacol. Sci.* **30,** 228–233
18. Yamashita, A., Singh, S. K., Kawate, T., Jin, Y., and Gouaux, E. (2005) Crystal structure of a bacterial homologue of Na^+/Cl^--dependent neurotransmitter transporters. *Nature* **437,** 215–223
19. Penmatsa, A., Wang, K. H., and Gouaux, E. (2013) X-ray structure of dopamine transporter elucidates antidepressant mechanism. *Nature* **503,** 85–90
20. Núñez, E., Alonso-Torres, P., Fornés, A., Aragón, C., and López-Corcuera, B. (2008) The neuronal glycine transporter GLYT2 associates with membrane rafts: functional modulation by lipid environment. *J. Neurochem.* **105,** 2080–2090
21. Park, E., and Rapoport, T. A. (2012) Mechanisms of Sec61/SecY-mediated protein translocation across membranes. *Annu. Rev. Biophys.* **41,** 21–40
22. Rutkevich, L. A., and Williams, D. B. (2011) Participation of lectin chaperones and thiol oxidoreductases in protein folding within the endoplasmic reticulum. *Curr. Opin. Cell Biol.* **23,** 157–166
23. Martinez-Maza, R., Poyatos, I., Lopez-Corcuera, B., Núñez, E., Giménez, C., Zafra, F., and Aragón, C. (2001) The role of *N*-glycosylation in transport to the plasma membrane and sorting of the neuronal glycine transporter GLYT2. *J. Biol. Chem.* **276,** 2168–2173
24. Arribas-González, E., Alonso-Torres, P., Aragón, C., and López-Corcuera, B. (2013) Calnexin-assisted biogenesis of the neuronal glycine transporter 2 (GlyT2). *PLoS One* **8,** e63230
25. Farhan, H., Freissmuth, M., and Sitte, H. H. (2006) Oligomerization of neurotransmitter transporters: a ticket from the endoplasmic reticulum to the plasma membrane. *Handb. Exp. Pharmacol.* 233–249
26. Chiba, P., Freissmuth, M., and Stockner, T. (2014) Defining the blanks: pharmacochaperoning of SLC6 transporters and ABC transporters. *Pharmacol. Res.* **83,** 63–73
27. Brown, T. C., Correia, S. S., Petrok, C. N., and Esteban, J. A. (2007) Functional compartmentalization of endosomal trafficking for the synaptic delivery of AMPA receptors during long-term potentiation. *J. Neurosci.* **27,** 13311–13315
28. Liu, Q. R., López-Corcuera, B., Mandiyan, S., Nelson, H., and Nelson, N. (1993) Cloning and expression of a spinal cord- and brain-specific glycine transporter with novel structural features. *J. Biol. Chem.* **268,** 22802–22808
29. Jimenez, E., Zafra, F., Perez-Sen, R., Delicado, E. G., Miras-Portugal, M. T., Aragon, C., and Lopez-Corcuera, B. (2011) P2Y purinergic regulation of the glycine neurotransmitter transporters *J. Biol. Chem.* **286,** 10712–10724
30. Geerlings, A., Núñez, E., Rodenstein, L., López-Corcuera, B., and Aragón, C. (2002) Glycine transporter isoforms show differential subcellular localization in PC12 cells. *J. Neurochem.* **82,** 58–65
31. de Juan-Sanz, J., Zafra, F., López-Corcuera, B., and Aragón, C. (2011) Endocytosis of the neuronal glycine transporter GLYT2: role of membrane rafts and protein kinase C-dependent ubiquitination. *Traffic* **12,** 1850–1867
32. Fernández-Sánchez, E., Díez-Guerra, F. J., Cubelos, B., Giménez, C., and Zafra, F. (2008) Mechanisms of endoplasmic-reticulum export of glycine transporter-1 (GLYT1). *Biochem. J.* **409,** 669–681
33. de Juan-Sanz, J., Núñez, E., Villarejo-López, L., Pérez-Hernández, D., Rodriguez-Fraticelli, A. E., López-Corcuera, B., Vázquez, J., and Aragón, C. (2013) Na^+/K^+-ATPase is a new interacting partner for the neuronal glycine transporter GlyT2 that downregulates its expression *in vitro* and *in vivo*. *J. Neurosci.* **33,** 14269–14281
34. Bolte, S., and Cordelières, F. P. (2006) A guided tour into subcellular colocalization analysis in light microscopy. *J. Microsc.* **224,** 213–232
35. Zafra, F., Gomeza, J., Olivares, L., Aragón, C., and Giménez, C. (1995) Regional distribution and developmental variation of the glycine transporters GLYT1 and GLYT2 in the rat CNS. *Eur. J. Neurosci.* **7,** 1342–1352
36. Núñez, E., Pérez-Siles, G., Rodenstein, L., Alonso-Torres, P., Zafra, F., Jiménez, E., Aragón, C., and López-Corcuera, B. (2009) Subcellular localization of the neuronal glycine transporter GLYT2 in brainstem. *Traffic* **10,** 829–843
37. de Juan-Sanz, J., Núñez, E., López-Corcuera, B., and Aragón, C. (2013) Constitutive endocytosis and turnover of the neuronal glycine transporter GlyT2 is dependent on ubiquitination of a C-terminal lysine cluster. *PLoS One* **8,** e58863
38. Nakatsukasa, K., and Brodsky, J. L. (2008) The recognition and retrotranslocation of misfolded proteins from the endoplasmic reticulum. *Traffic* **9,** 861–870
39. Sucic, S., Koban, F., El-Kasaby, A., Kudlacek, O., Stockner, T., Sitte, H. H., and Freissmuth, M. (2013) Switching the clientele: a lysine residing in the C terminus of the serotonin transporter specifies its preference for the coat protein complex II component SEC24C. *J. Biol. Chem.* **288,** 5330–5341
40. Pettit, R. S. (2012) Cystic fibrosis transmembrane conductance regulator-modifying medications: the future of cystic fibrosis treatment. *Ann. Pharmacother.* **46,** 1065–1075
41. Leidenheimer, N. J., and Ryder, K. G. (2014) Pharmacological chaperoning: a primer on mechanism and pharmacology. *Pharmacol. Res.* **83,** 10–19
42. López-Corcuera, B., Vázquez, J., and Aragón, C. (1991) Purification of the sodium- and chloride-coupled glycine transporter from central nervous system. *J. Biol. Chem.* **266,** 24809–24814
43. Engin, F., and Hotamisligil, G. S. (2010) Restoring endoplasmic reticulum function by chemical chaperones: an emerging therapeutic approach for metabolic diseases. *Diabetes Obes. Metab.* **12,** 108–115
44. Lindquist, S. L., and Kelly, J. W. (2011) Chemical and biological approaches for adapting proteostasis to ameliorate protein misfolding and aggregation diseases: progress and prognosis. *Cold Spring Harb. Perspect. Biol.* 10.1101/cshperspect.a004507
45. Ghavami, S., Shojaei, S., Yeganeh, B., Ande, S. R., Jangamreddy, J. R., Mehrpour, M., Christoffersson, J., Chaabane, W., Moghadam, A. R., Kashani, H. H., Hashemi, M., Owji, A. A., and Łos, M. J. (2014) Autophagy and apoptosis dysfunction in neurodegenerative disorders. *Prog. Neurobiol.* **112,** 24–49
46. Iannitti, T., and Palmieri, B. (2011) Clinical and experimental applications of sodium phenylbutyrate. *Drugs R. D.* **11,** 227–249
47. Merulla, J., Fasana, E., Soldà, T., and Molinari, M. (2013) Specificity and regulation of the endoplasmic reticulum-associated degradation machinery. *Traffic* **14,** 767–777
48. Deleted in proof
49. Bartholomäus, I., Milan-Lobo, L., Nicke, A., Dutertre, S., Hastrup, H., Jha, A., Gether, U., Sitte, H. H., Betz, H., and Eulenburg, V. (2008) Glycine transporter dimers: evidence for occurrence in the plasma membrane. *J. Biol. Chem.* **283,** 10978–10991
50. Ron, D., and Walter, P. (2007) Signal integration in the endoplasmic reticulum unfolded protein response. *Nat. Rev. Mol. Cell Biol.* **8,** 519–529
51. Fujiwara, M., Yamamoto, H., Miyagi, T., Seki, T., Tanaka, S., Hide, I., and Sakai, N. (2013) Effects of the chemical chaperone 4-phenylbutylate on the function of the serotonin transporter (SERT) expressed in COS-7 cells. *J. Pharmacol. Sci.* **122,** 71–83
52. Ozcan, L., Ergin, A. S., Lu, A., Chung, J., Sarkar, S., Nie, D., Myers, M. G., Jr., and Ozcan, U. (2009) Endoplasmic reticulum stress plays a central role in development of leptin resistance. *Cell Metab.* **9,** 35–51